

Complex reactions on a convertible catalyst surface: A study of the S-O-Cu system

S. Dürrbeck^{a,b}, X.-R. Shi^c, M. Samadashvili^{b,1}, J. Redinger^d, E. Bertel^{a,*}, M. Salmeron^{b,*}

^a Institute of Physical Chemistry, University of Innsbruck, Austria

^b Lawrence Berkeley Laboratory, Berkeley, CA, United States

^c College of Materials Engineering, Shanghai University of Engineering Science, Shanghai 201620, PR China

^d Department of Applied Physics, Vienna University of Technology, Austria

ARTICLE INFO

Keywords:

Catalysis

Sulphur

Copper

Scanning tunnelling microscopy

Density functional theory

ABSTRACT

The interaction of clean and partially oxidized Cu(110) with sulphur was studied by scanning tunneling microscopy and density functional theory calculations in the low-coverage range. On the clean Cu surface individual S atoms adsorb in the troughs between the Cu atom rows. Hollow sites are preferred, but long-bridge sites are occasionally occupied as well. The majority of adsorbed S, however, seems to be involved in the formation of highly mobile Cu_xS_y clusters of various sizes. The clusters preferentially attach to steps thus changing the step morphology completely. Some of the clusters form aggregates on the terraces. On the partially oxidized surface similar clusters form and cause long-range mass transport to steps. Additionally, nanowires form in [001] direction on and along the surface oxide stress domains. These nanowires have a complex composition, exhibit different corrugations and appear sometimes as three-dimensional needles. Occasionally they flip their direction by 90°, but doing so they partially decompose. Finally, annealing of the S-O-Cu surface leads to consumption of the surface oxide stripes indicating loss of oxygen presumably via SO₂ formation. Simultaneously, linear sulphur chains suspended between the [001] –O-Cu-O– chains form in [110] direction. The surprising multitude of processes and products even at low-pressure, low-temperature conditions in the comparatively simple S-O-Cu system highlights the difficulty of controlling reactivity and selectivity on such convertible catalyst surfaces.

1. Introduction

Copper catalyzes a number of industrially important chemical reactions. It is used for instance as desulfurization catalyst [1,2], in the low-temperature stage of the water gas shift reaction [3,4] and in (electro)catalytic CO₂ reduction [5,6]. The catalytic activity of copper can in part be attributed to its electronic structure [7], but morphology, e.g. number density and type of under-coordinated sites etc. is an important descriptor as well [8]. The Sulfur-Cu interaction has been addressed in several previous surface science studies, both experimentally [9–20] and theoretically [21–25]. Interest in this system arises not only from the use of Cu as desulfurization catalyst, but also from the S poisoning of the water gas shift reaction. S induced corrosion of Cu plays an important role in the deterioration of cultural artefacts and is relevant for nuclear waste disposal, since the radioactive waste is sometimes confined in copper containers [25]. In the present study we revisit the interaction of Cu(110) and partially oxidized Cu(110) with Sulfur by scanning tunneling microscopy (STM). In contrast to the

majority of previous investigations we dose pure S onto Cu(110). We expected this to simplify the surface reactions in comparison to SO₂ or H₂S exposure, since disproportionation reactions and hydroxyl or water formation should be suppressed in this case. Surprisingly, an extremely complex variety of surface reactions is observed with mobile cluster formation, long-distance mass transport, and most notably formation of different minority species, which will be very difficult to identify by spectroscopic methods and yet may be important reaction intermediates in catalytic processes.

2. Experiment and theory

The experiments have been carried out in a UHV system featuring a preparation chamber and a separate cryostat chamber housing the STM. The preparation chamber was equipped with a solid-state electrolysis cell for sulfur dosing [26]. Exposures to both, S and O₂, were carried out at room temperature, whereas the STM images were recorded at 77 K. In the following, we give the sulfur dose in atoms per

* Corresponding authors.

E-mail address: erminald.bertel@uibk.ac.at (E. Bertel).

¹ Present address: Tbilisi, Georgia.

<https://doi.org/10.1016/j.susc.2018.03.010>

Received 26 January 2018; Received in revised form 27 February 2018; Accepted 17 March 2018

0039-6028/ © 2018 Elsevier B.V. All rights reserved.

cm^2 . Global sulfur coverages are of little significance since we observe immediate attack of the S at Cu step edges, mobile clusters and three-dimensional (3D) growth, i.e. extremely inhomogeneous local S coverage. Long-range ordered overlayers formed only after large exposures, but the present investigation is focused on the lower coverage range, where the Cu surface is still well defined and a variety of structures is observed.

The calculations were performed with plane-wave density functional theory (DFT) using the Vienna ab initio simulation package (VASP) [27,28]. Potentials within the projector augmented wave method (PAW) [29] and the generalised gradient approximation (GGA) with the Perdew-Wang 91 functional were used [30]. For bulk optimization, the lattice parameters were obtained by minimizing the total energy of the unit cell using a conjugated gradient algorithm to relax the ions and considering a set of $4 \times 4 \times 4$ Monkhorst-Pack k-points to sample the Brillouin Zone. Cu(110) surfaces were modelled with slabs of five layer thicknesses. During optimization, the top three layers together with the adsorbed species were allowed to relax, and a set of $1 \times 2 \times 1$ Monkhorst-Pack k-points was used for the (4×4) surface unit cell. A kinetic energy cutoff of 400 eV was employed for all the calculations.

3. Results and discussion

Three major changes occur at the Cu(110) surface upon S dosing. Bright islands appear with frizzy edges. This indicates the presence of a mobile species at room temperature, which tends to form islands. The islands have different sizes, variable shapes and seem to be mobile even at the measuring temperature of 77 K. From Fig. 1A one can conclude that they move preferentially along the $[1\bar{1}0]$ direction.

Secondly, dark rings with bright centres in trough sites are observed. Comparison with contours of constant local density of states (LDOS) obtained from a DFT calculation of the (2×2) -S/Cu(110) system (inset in Fig. 1) identifies these features as atomic S species. For

atomic S, the hollow site (H) is the most stable one [9,21], but the long-bridge site (LB) is only slightly higher in energy. In Fig. 1B a grid is locally superimposed with the gridpoints centred at the Cu surface atoms. Although the individual Cu atoms are not resolved in Fig. 1B, the STM length scale can be accurately calibrated from the Cu row distances and cross-checked with the dimensions of the Cu-O stripes of the partially oxidised surface. This leaves only the lateral positioning of the grid for adjustment. Here, the grid has been aligned in such a way that the majority of the sulphur atoms is located in the more stable H site. Quite clearly, however, some occupied LB sites are found as well.

The third change brought about by S exposure is particularly evident, if the exposure is increased significantly beyond the one for Fig. 1A–C. Fig. 1D shows the surface morphology after an exposure of 2.18×10^{14} atoms/ cm^2 . The steps are no longer parallel to the $[1\bar{1}0]$ direction as they largely still are in Fig. 1C. Apparently, a mass transport involving Cu atoms has occurred and the step energy has become more isotropic, as one should expect for the presence of an adsorbate, which gains excess binding energy on a step or kink site relative to a terrace site. The Cu mass transport suggests that Cu atoms are involved in the formation of the mobile bright islands. This conforms to the well-known tendency of Cu surfaces to form extremely mobile Cu_xS_y clusters reported for other low-index Cu surfaces [10–12,23]. Carley et al. [13] studied the adsorption of H_2S on Cu(110) by room temperature STM and concluded indirectly from the change in step morphology that mobile S-Cu complexes are formed. They were not able to identify individual S atoms, which they attributed to a high mobility of this species at 295 K. In contrast to their room temperature study, the present 77 K data provide direct evidence for both, mobile clusters and individual chemisorbed S atoms. High mobility of Cu atoms detaching from steps due to CO adsorption in dynamic equilibrium with CO gas (in the Torr regime) was also observed in a previous study [31].

Fig. 2 shows the adsorption of S on an oxygen pre-dosed Cu(110) surface. The oxygen coverage is slightly below 0.25 monolayers (ML). 0.5 ML corresponds to a uniform $\text{O}(2 \times 1)$ -Cu(110) surface [32]. At

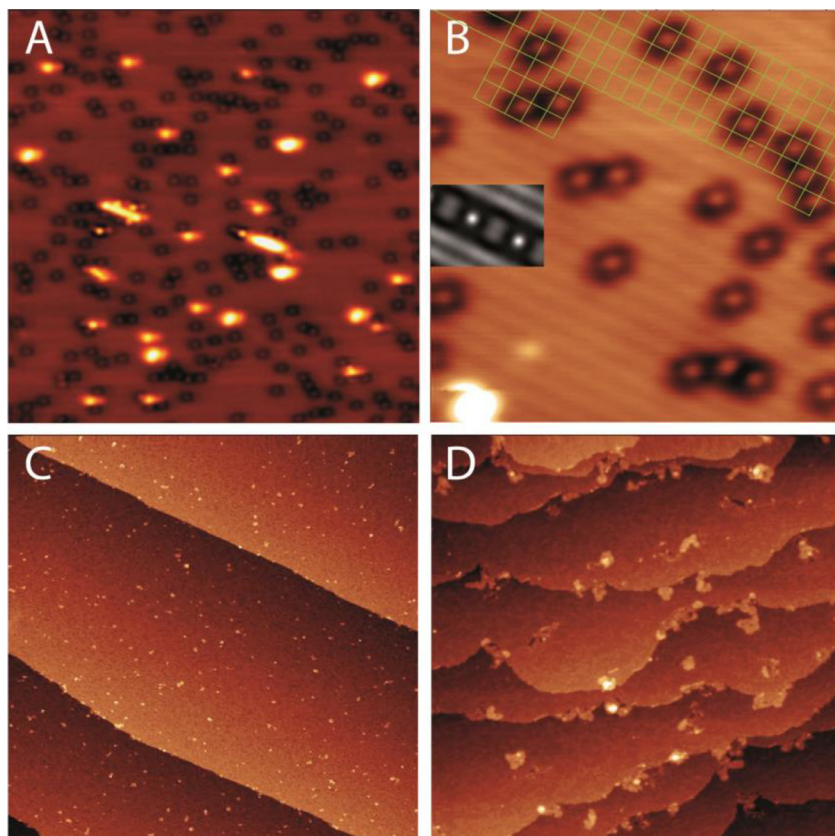


Fig. 1. A: Clean Cu(110) surface exposed to 3.12×10^{13} atoms/ cm^2 (the actual coverage presumably being significantly smaller). Two species are observed: dark rings around bright centers and bright islands with somewhat frizzy edges. (20×20 nm 2 ; U_{bias} : -25 mV, I_t : 50 pA). B: Same preparation as A, but annealed to 373 K. The grid in the upper part marks the positions of the Cu atoms on the Cu(110) surface (7.3×7.3 nm 2 ; U_{bias} : 30 mV, I_t : 150 pA). The inset shows a DFT simulation of the STM contrast for a (4×4) -S/Cu(110) adsorption layer with tip-sample distance at 2 Å. C: Large-scale image of the same preparation as B. (280×280 nm 2 ; U_{bias} : 500 mV, I_t : 50 pA). D: Clean Cu(110) surface exposed to 2.18×10^{14} atoms/ cm^2 (140×140 nm 2 ; U_{bias} : 50 mV, I_t : 50 pA).

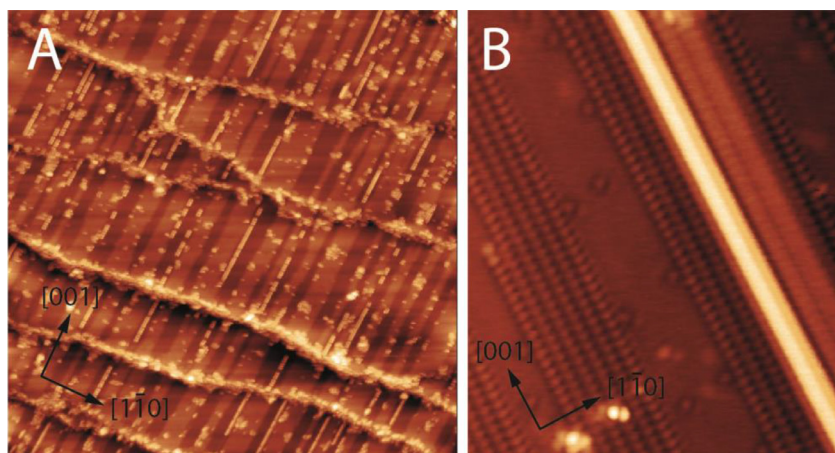


Fig. 2. A: Sulphur adsorption on 0.2 ML O(2×1)-Cu(110) (Exposure approx. 6×10^{12} atoms/cm²). The dark stripes are the surface oxide stress domains, bright patches and lines appear upon S adsorption (140×140 nm²; U_{bias} : -500 mV, I_t : 70 pA). B: High-resolution image of a similar preparation as in A (12.3×14.9 nm²; U_{bias} : 300 mV, I_t : 100 pA).

lower coverages a regular array of stress domains forms, the so-called piano-board surface structure. The origin of this name is evident from Fig. 2A, where the O(2×1) stress domains appear as dark stripes crossing the terraces from step to step. S adsorption causes two features to appear: First, clusters, which form more or less exclusively on the clean Cu stripes, but preferentially at the edges of the surface oxide stripes. Clearly, the edges of the surface oxide domains are sites of enhanced chemical activity. Second, long chains or nanowires form within the oxide stripes. The stripes themselves remain unaltered. Apparently, at this stage there is no significant reaction with oxygen. Post-adsorption of oxygen did not change the overall pattern: the stress domains formed almost the same way as on the clean surface. This is in remarkable contrast to the study of Carley et al. [13], where H₂S pre-adsorption blocked the formation of surface oxide stripes. The present results suggest that this is not due to the presence of sulfur, but that the hydrogen reacts at 298 K with the surface oxygen to form hydroxyl groups or even water thus significantly changing the surface chemistry, in contrast to the clean Cu surface [33].

The overall pattern remains almost unchanged, if the Cu/O/S surface is heated to 323 K after S exposure. However, during annealing to 373 K, dramatic changes occur (see Fig. 3). The steps on the surface become much more serrated (Fig. 3A). Higher resolution images (Fig. 3C and D) reveal an alteration of the CuO stripes, which are partially consumed. Instead new chains form along the $[1\bar{1}0]$ direction. Fig. 3C provides atomic resolution of the Cu atoms in the clean Cu patches thus allowing to gauge the periodicity of the $[1\bar{1}0]$ chains: they exhibit a periodicity of 255 pm, corresponding to the Cu nearest-neighbour (nn) distance.

The copper atoms liberated during the consumption of the oxide stripes are apparently only partially, if at all, incorporated into the $[1\bar{1}0]$ chains, since the step morphology changes considerably during the process indicating that the majority of the Cu atoms is travelling to the steps. The resulting outward growth of the steps causes all the remaining oxide stripes to end on the terraces before reaching the steps as seen in Fig. 3A. Presumably, the high mobility of the Cu is attributable to Cu_xS_y clusters similar to those seen on the pure Cu surface [10–12,23].

In addition to the long-range transport and the short chains oriented along the $[1\bar{1}0]$ direction, nanowires in $[001]$ direction can be seen e.g. in Figs. 3D and 4. These nanowires are not to be confused with single -O-Cu-O- chains remaining from the consumption of the O(2×1)-Cu stress domains, as they appear for instance in Fig. 3C. The $[001]$ nanowires are always attached to CuO chains or domains. They are similar to the nanowires formed in the surface oxide domains shown in Fig. 2B. In some cases the flipping of a complete nanowire, originally aligned on the oxide stripes in $[001]$ direction, into the $[1\bar{1}0]$ direction could be observed (see Fig. 4). Of course it cannot be excluded that the flipping is triggered by the STM tip, although the tunnelling conditions are quite

mild ($U_{\text{bias}} = 35$ mV, I_t : 50 pA), but the at least partial internal coherence of the structure is remarkable.

The morphology appearing in Fig. 3B is reminiscent of that observed by Alemozafar et al. in their adsorption studies of SO₂ on Cu(110) [15,17]. However, closer inspection reveals fundamental differences: First, in their images recorded after SO₂ adsorption on the piano-board structure nanowires in $[001]$ direction are absent. This should be compared to Figs. 2A, 3A, 3D and 4, where such nanowires are a sparsely dispersed, but prominent feature. More importantly, the $[1\bar{1}0]$ chains formed between the oxide stripes after SO₂ exposure have a twofold periodicity and form occasionally a local $p(2 \times 2)$ configuration. Here, after S exposure, the $[1\bar{1}0]$ chains have the periodicity of the underlying Cu rows, i.e. 255 pm (see Fig. 3C). Fig. 5 shows high-resolution images of such a chain obtained with two different tip conditions and revealing further details: The building blocks seem to be asymmetric, with the orientation switching at a certain position within the chain (arrow in Fig. 5A).

From their XPS and temperature-programmed reaction spectroscopy data including isotope labelling Alemozafar et al. [15–17] concluded that SO₂ reacts with the surface oxygen to form SO₃(ads) in a monodentate bonding configuration. Consequently, they assumed the $[1\bar{1}0]$ chains to consist of SO₃ moieties residing in hollow sites. They also found these chains to migrate via collective motion. The $[1\bar{1}0]$ chains observed here are also located in the troughs between the top-layer copper rows and they are also mobile to some extent (see Fig. 3C, where the $[1\bar{1}0]$ chain seems to change position while the image is recorded). Despite a superficial similarity to the results of Alemozafar et al. [15,17], the chains forming in the present experiment cannot consist of SO₃ building blocks. The periodicity does not agree and indeed, according to our DFT results, it is impossible to arrange SO₃ units at such a packing density as obtained here. Further details about the $[1\bar{1}0]$ chains can be derived from Fig. 5, where images are compared which have been recorded with different states of the STM tip. In Fig. 5A the Cu atoms in the oxide CuO chains are imaged as protrusions, while in Fig. 5B the oxygen atoms appear as hills. The $[1\bar{1}0]$ chain shows the same contrast behaviour as the oxygen atoms and it contains very closely packed atoms with a periodicity of 255 pm. This together with the known tendency of S to form S_x chains leads us to suggest that the $[1\bar{1}0]$ chains are linear S aggregates. The S–S bond is known to be rather flexible and bond length between 180 and 300 pm are possible depending on the configuration and the ligands [34]. The conspicuous asymmetry seen in Fig. 5A might argue against a simple atomic chain, but it could stem from an asymmetric adsorption site rather than an asymmetry of the constituents. With identical building blocks and the chain being suspended between -O-Cu-O- added rows, asymmetric adsorption sites would seem unlikely. However, asymmetric S chains are known to exist [35] and to be only marginally different in energy in relation to symmetric ones. Steudel and Steudel [35] interpret them as

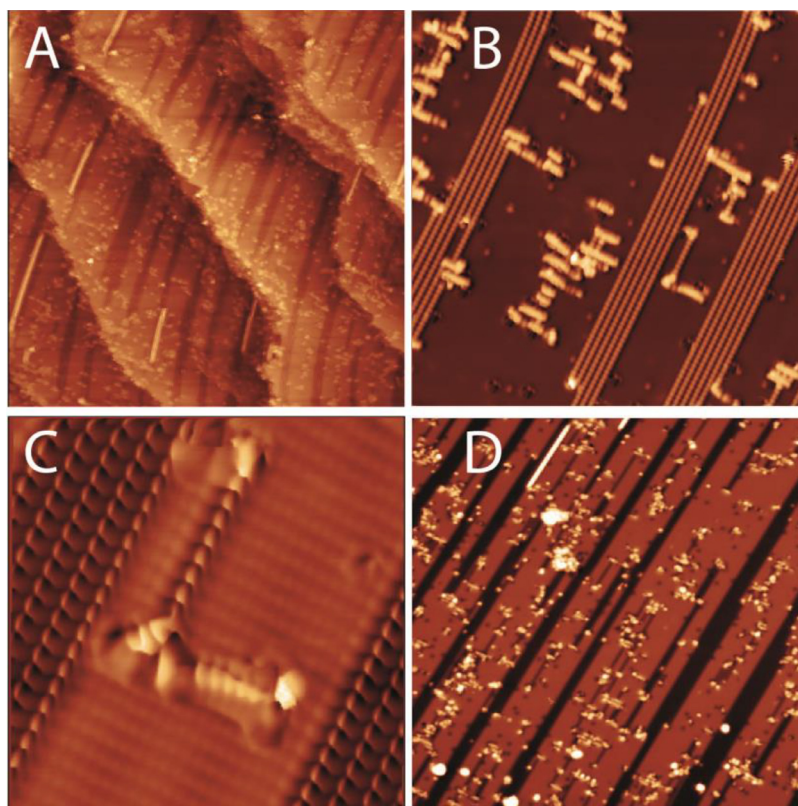


Fig. 3. A: S on $0.2 \text{ ML O}(2 \times 1)\text{-Cu}(110)$ similar to Fig. 2A, but after annealing to 373 K ($112 \times 112 \text{ nm}^2$; $U_{\text{bias}} = -50 \text{ mV}$, I_t : 70 pA). B: High-resolution image as in A, showing the formation of $[1\bar{1}0]$ chains ($28 \times 28 \text{ nm}^2$; $U_{\text{bias}}: -200 \text{ mV}$, I_t : 35 pA). C: High-resolution image of the structure seen in the lower right of B, showing the remnant of an O-Cu-O chain from the surface oxide stripes and attached to it a $[1\bar{1}0]$ chain ($7 \times 7 \text{ nm}^2$; $U_{\text{bias}}: -10 \text{ mV}$, I_t : 35 pA). In B and C imaging conditions are such that the Cu and the O, respectively, in the O-Cu-O chains is imaged as protrusion. D: Overview of the same preparation after annealing to 423 K ($70 \times 70 \text{ nm}^2$; $U_{\text{bias}}: 100 \text{ mV}$, I_t : 50 pA).

an adduct between S_n^- and S_m . This would nicely fit the morphology of the $[1\bar{1}0]$ chain shown in Fig. 5A. The problem with the $S_n^-S_m$ adduct chain is on the one hand, whether such an asymmetric chain would survive on the Cu surface. On the other hand, an asymmetric charge distribution is plausible, since the chain is confined on one side by a regular $\text{O}(2 \times 1)\text{-Cu}(110)$ stripe, while on the other side it is attached to a short single -O-Cu-O- chain terminated at least on one side by a Cu atom or a Cu containing cluster. Furthermore, the centre of inversion (black arrow in Fig. 5), looks very similar to the rest of the chain and shows the same contrast inversion upon tip change. This supports an assignment as S atom with only different bond length from the rest of the chain.

Notably, the $[1\bar{1}0]$ chains form only in the presence of the Cu-O-Cu chains in the Cu surface oxide and the surface oxide stripes are consumed during the formation of the chains. This suggests the following scenario: Since the $[1\bar{1}0]$ chains can contain, if at all, only very little oxygen, the oxygen is apparently reacted away during the annealing to 100°C . Most likely, this occurs via oxidation of S: $\text{S} + \text{O} \rightarrow \text{SO}$; $\text{SO} + \text{O} \rightarrow \text{SO}_2$. SO has been shown to be a short-lived reaction intermediate, not observable for instance in XPS [14,17]. SO_2 is weakly adsorbed and can desorb during the annealing step at 100°C . The Cu atoms liberated in the Cu surface-oxide consumption form Cu_xS_y clusters and travel to the steps. Some of the adsorbed S clusters (the distribution of S species emitted from the source depends critically on the

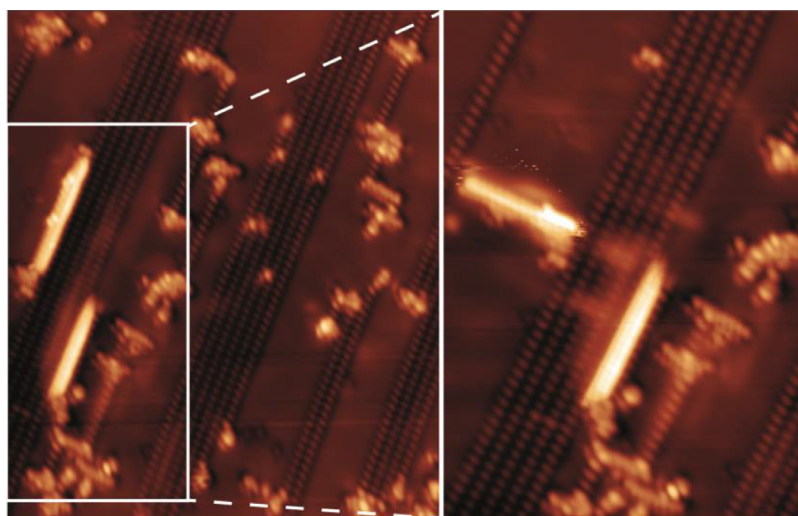


Fig. 4. Back-to-back recorded images show an entire $[001]$ nanowire flipping over into a $[1\bar{1}0]$ chain, albeit with some reconfiguration: Only part of the nanowire retains its original internal structure, while some of the material originally forming the double chain is spread out around the chain. (Exposure approx. 6×10^{12} atoms/ cm^2 ; left: $20.4 \times 24 \text{ nm}^2$; $U_{\text{bias}}: 50 \text{ mV}$, I_t : 20 pA; right: $12 \times 16 \text{ nm}^2$; $U_{\text{bias}}: 35 \text{ mV}$, I_t : 50 pA).

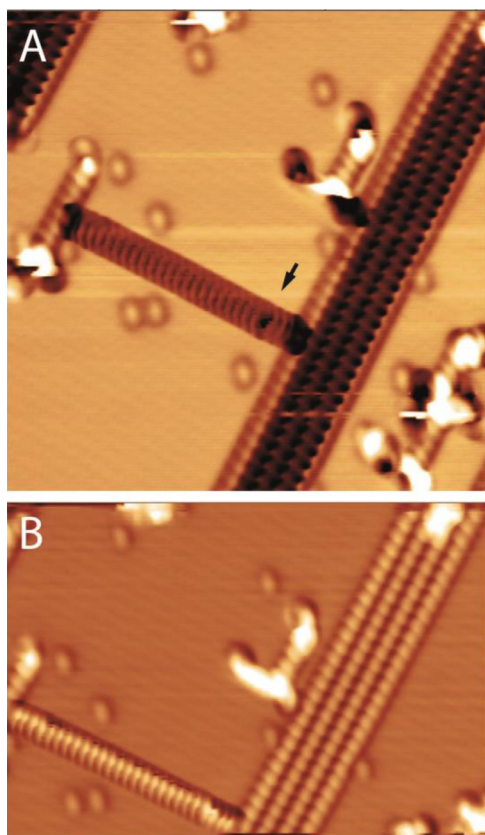


Fig. 5. A: High-resolution image of a typical $[1\bar{1}0]$ chain. The chain periodicity is 255 pm. Note the asymmetric shape of the building blocks and the mirror symmetry around a defect site within the chain (arrow). Cu atoms appear as protrusions. The chain is aligned along a trough of the Cu substrate and exhibits a periodicity of 255 pm, i.e. the same periodicity as the close-packed Cu rows on clean Cu(110). ($12.8 \times 12.8 \text{ nm}^2$; U_{bias} : 25 mV, I_t : 50 pA). B: After a change in the tip condition, the contrast is inverted. Now the oxygen atoms are imaged as protrusions. ($12.8 \times 8.3 \text{ nm}^2$; U_{bias} : 25 mV, I_t : 50 pA).

temperature and is not well known) form the $[1\bar{1}0]$ chains. Stabilisation of the chains requires a terminating $\text{Cu}^{\delta+}$. Therefore, the $[1\bar{1}0]$ chains are most of the time suspended between $-\text{O}-\text{Cu}-\text{O}-$ chains (in Fig. 3C one end seems to be terminated by a Cu_xS_y cluster).

It is much more difficult to find a plausible model for the $[001]$

nanowires formed during low-T exposure within or alongside the Cu surface-oxide stripes (Figs. 2, 3A, 3D, 4, and 6). They are not entirely uniform, sometimes appearing with (Fig. 6A), sometimes without an inner structure (Fig. 6B). They are present after S dosing onto the partially oxidised Cu surface at 298 K (Fig. 6A and B) and survive annealing to 323 K and 423 K (Fig. 4). In Fig. 4 it is shown that even at 77 K such a nanowire can flip its direction, but during this process it partially decomposes, presumably shedding off Cu_xS_y clusters. In some cases at least, the nanowire islands are apparently more than one monolayer in height, as shown in Fig. 6A and C. The profile in Fig. 6C, however, should not be mistaken as reflecting the true geometry, since it depends on the tip state and the conductivity of the structure. Note that with the tip state in Fig. 6 the oxide stripes appear as depressions, i.e. lower than the surrounding clean Cu surface in contrast to the actual geometry. As these nanowires are a minority species coexisting with Cu_xS_y clusters and $-\text{O}-\text{Cu}-\text{O}-$ chains and seem to contain Cu, O and S in various compositions, it will be extremely difficult to elucidate their precise structure with any spectroscopy.

A series of DFT calculations was carried out in order to support the interpretation of at least some of the surface reaction products. The identification of single adsorbed S atoms is rather convincing in view of the peculiar contrast with a central protrusion and a surrounding dark ring. We did not try to elucidate the detailed structure of the mobile Cu_xS_y clusters, since they apparently vary in size, shape and mobility (see Fig. 1) and a unique identification on the basis of energetics alone is hardly possible [11]. Thus our efforts focused on a model for the $[1\bar{1}0]$ chains shown in Fig. 5. We first followed the suggestion of Alemozafar et al. [15,17] trying to construct the chains from Cu and SO_3 building units or from SO_3 alone. No reasonable geometry was found with a single periodicity, since strong repulsive interactions prevented any stable arrangement.

Next we tried chain structures with a Cu backbone of single-periodicity connected to S atoms in either CuS, Cu_2S_3 or CuS_3 stoichiometry based on the assumption that S atoms in various bridging geometries could account for the internal stability of the chains. The geometry optimization, however, invariably resulted in a decay of the chains into its atomic constituents with the latter finally occupying high-symmetry sites. Thus neither the characteristic asymmetry nor the internal bonding along the chain direction responsible for the collective motion could be reproduced. Finally we investigated chains with S backbones and O atoms in various bonding configurations. In the dense geometry required for a chain with single-periodicity the least repulsive interactions occurred for a 1:1 stoichiometry. Single (OSO) and double chains (OSSO) [36] were examined. In the latter case, a weak attractive

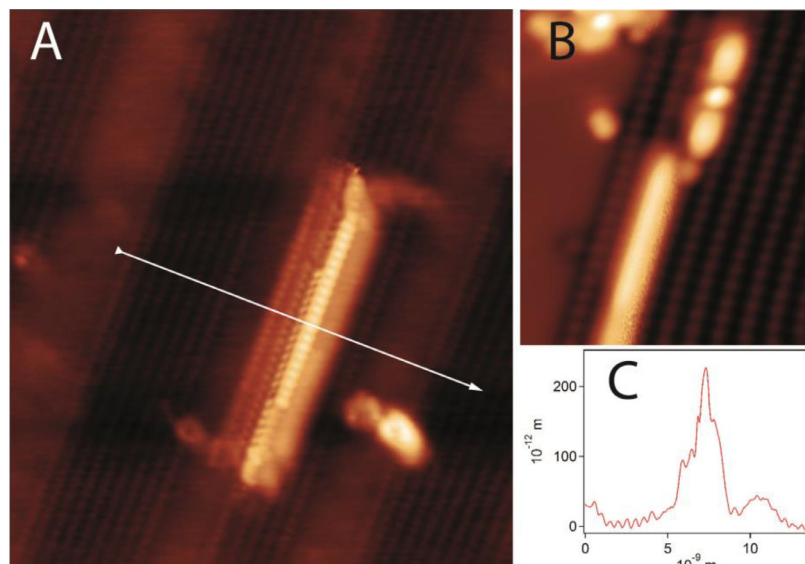


Fig. 6. A: Nanowire structure in $[001]$ direction formed after S exposure on a $(2 \times 1)\text{O}-\text{Cu}(110)$ stripe. ($18 \times 20 \text{ nm}^2$; U_{bias} : 300 mV, I_t : 200 pA) B: A different type of $[001]$ nanowire, where no internal structure could be resolved. ($3.8 \times 4.3 \text{ nm}^2$; U_{bias} : -250 mV, I_t : 50 pA). C: Profile of the nanowire shown in A.

interaction between OSSO units occurred at distances between 600 pm and 460 pm, but quickly changed to repulsive upon further compression. Furthermore, the chains tended to disintegrate into SO units, which adsorbed in a flat geometry in $[1\bar{1}0]$ direction, thus excluding a single periodicity. Chains consisting of sulphur rings with attached oxygen did not match the required single periodicity. In addition, once adsorbed on the Cu(110) surface they tended to decay into S chains. The S chains obtained in the DFT calculations, while consistent with the required periodicity, were always symmetric. Thus we were finally led to the present proposal of an asymmetric S chain or, in other words, an $S_n^-S_m$ adduct chain, where the asymmetry is caused by a different termination at opposite ends. Such a configuration is of course hard to model in a DFT calculation, because it requires very large unit cells for modelling the different terminating Cu-O, resp. Cu-S-O species.

4. Summary

Even under UHV conditions and moderate temperatures the interaction of Cu(110) with S gives rise to a variety of restructuring processes. Formation of highly mobile Cu_xS_y clusters results in long-range mass transport and complete change of step morphology. Some of the clusters coalesce to form islands on the terraces. Individual S atoms appear as well as statistically distributed adsorbates in the troughs between the Cu rows on clean Cu terraces. Long-bridge and hollow sites are both occupied with a slight preference for the latter. On partially oxidised Cu(110) complex nanowire structures oriented in $[001]$ direction appear randomly on and at the surface oxide stripes. Occasionally they flip into the $[1\bar{1}0]$ direction, but this is associated with partial decomposition. If the surface is annealed to 423 K the surface oxide stripes are progressively consumed with increasing sulfur exposure. Apparently some of the oxygen is reacted away via SO_2 desorption. Additionally, chains with a periodicity of 255 pm are formed in $[1\bar{1}0]$ direction. Testing several models for these chains by DFT calculations led us finally to attribute these structures to linear S_x species terminated by $Cu^{\delta+}$ atoms within $-O-Cu-O-$ chains. An asymmetric termination then gives rise to asymmetric chains. Each of the observed structures might result in different reaction paths in a catalytic process. Thus the present results illustrate once more the complexity of catalytic reactions even under well-controlled conditions in a low-pressure, low-temperature environment. Finally, the reactions observed here might also be relevant for the S induced transport processes in lithium-sulphur battery systems.

Acknowledgement

This work was supported by the Office of Basic Energy Sciences (BES), Division of Materials Sciences and Engineering, of the U.S. Department of Energy (DOE) under contract no. DE-AC02-05CH11231, through the Structure and Dynamics of Materials Interfaces (FWP KC31SM) program. E.B. and S.D. wish to thank the University of Innsbruck for financial support during their stay at the Lawrence Berkeley Laboratory. X.-R.S. is sponsored by the Shanghai Pujiang Program (17PJ1403100) and the National Natural Science Foundation of China (21703137).

References

- [1] J.N. Armor, Environmental catalysis, Appl. Catal. B: Environ. 1 (1992) 221–256.
- [2] A.J. Hernández-Maldonado, R.T. Yang, Desulfurization of diesel fuels by adsorption via π -complexation with vapor-phase exchanged Cu(I)–Y zeolites, J. Am. Chem. Soc. 126 (2004) 992–993.
- [3] S. Pradhan, A.S. Reddy, R.N. Devi, S. Chilukuri, Copper-based catalysts for water gas shift reaction: Influence of support on their catalytic activity, Catal. Today 141 (2009) 72–76.
- [4] K. Kochloeff, Water gas shift and COS removal (Ed.), in: G. Ertl, H. Knözinger, J. Weitkamp (Eds.), Handbook of Heterogeneous Catalysis, Wiley-VCH, Weinheim, 1997, p. 1836.
- [5] M. Favaro, H. Xiao, T. Cheng, W.A. Goddard, J. Yano, E.J. Crumlin, Subsurface

- oxide plays a critical role in CO_2 activation by Cu(111) surfaces to form chemisorbed CO_2 , the first step in reduction of CO_2 , Proc. Natl. Acad. Sci. 114 (2017) 6706–6711.
- [6] A. Eilert, F. Cavalca, F.S. Roberts, J. Osterwalder, C. Liu, M. Favaro, E.J. Crumlin, H. Ogasawara, D. Friebe, L.G.M. Pettersson, A. Nilsson, Subsurface oxygen in oxide-derived copper electrocatalysts for carbon dioxide reduction, J. Phys. Chem. Lett. 8 (2017) 285–290.
- [7] A.A. Peterson, F. Abild-Pedersen, F. Studt, J. Rossmeisl, J.K. Nørskov, How copper catalyzes the electroreduction of carbon dioxide into hydrocarbon fuels, Energy Environ. Sci. 3 (2010) 1311–1315.
- [8] W. Tang, A.A. Peterson, A.S. Varela, Z.P. Jovanov, L. Bech, W.J. Durand, S. Dahl, J.K. Nørskov, I. Chorkendorff, The importance of surface morphology in controlling the selectivity of polycrystalline copper for CO_2 electroreduction, Phys. Chem. Chem. Phys. 14 (2012) 76–81.
- [9] A. Atrei, A.L. Johnson, D.A. King, Sulphur adsorption on Cu(110): a SEXAFS study, Surf. Sci. 254 (1991) 65–72.
- [10] J.W. Evans, P.A. Thiel, A little chemistry helps the big get bigger, Science 330 (2010) 599–600.
- [11] H. Walen, D.-J. Liu, J. Oh, H. Lim, J.W. Evans, C.M. Aikens, Y. Kim, P.A. Thiel, Cu_2S_3 complex on Cu(111) as a candidate for mass transport enhancement, Phys. Rev. B 91 (2015) 045426.
- [12] D.-J. Liu, H. Walen, J. Oh, H. Lim, J.W. Evans, Y. Kim, P.A. Thiel, Search for the structure of a sulfur-induced reconstruction on Cu(111), J. Phys. Chem. C (2014), <http://dx.doi.org/10.1021/jp505351g>.
- [13] A.F. Carley, P.R. Davies, R.V. Jones, K.R. Harikumar, G.U. Kulkarni, M.W. Roberts, The structure of sulfur adlayers at Cu(110) surfaces: an STM and XPS study, Surf. Sci. 447 (2000) 39–50.
- [14] H. Lu, E. Janin, M.E. Dávila, C.M. Pradier, M. Göthelid, Adsorption of SO_2 on Cu(100) and Cu(100)-c(2×2)-O surfaces studied with photoelectron spectroscopy, Vacuum 49 (1998) 171–174.
- [15] A.R. Alemozafar, X.-C. Guo, R.J. Madix, Collective motion and oscillatory interaction: $-Cu-O-$ and sulfite on Cu(110), Surf. Sci. 526 (2003) L127–L132.
- [16] A.R. Alemozafar, X.-C. Guo, R.J. Madix, Topographic nano-restructuring: sulfur dioxide adsorption on Cu(110), Surf. Sci. 524 (2003) L84–L88.
- [17] A.R. Alemozafar, X.-C. Guo, R.J. Madix, Adsorption and reaction of sulfur dioxide with Cu(110) and Cu(110)-p(2×1)-O, J. Chem. Phys. 116 (2002) 4698–4706.
- [18] T. Nakahashi, S. Terada, T. Yokoyama, H. Hamamatsu, Y. Kitajima, M. Sakano, F. Matsui, T. Ohta, Adsorption of SO_2 on Cu(100) studied by X-ray absorption fine structure spectroscopy and scanning tunneling microscopy, Surf. Sci. 373 (1997) 1–10.
- [19] W.L. Ling, N.C. Bartelt, K. Pohl, J. de la Figuera, R.Q. Hwang, K.F. McCarty, Enhanced self-diffusion on Cu(111) by trace amounts of S: chemical-reaction-limited kinetics, Phys. Rev. Lett. 93 (2004) 166101.
- [20] C.T. Campbell, B.E. Koel, $H_2S/Cu(111)$: a model study of sulfur poisoning of water-gas shift catalysts, Surf. Sci. 183 (1987) 100–112.
- [21] G. Lanzani, K. Laasonen, SO_2 and its fragments on a Cu(110) surface, Surf. Sci. 602 (2008) 321–344.
- [22] P.N. Abufager, P.G. Lustemberg, C. Crespos, H.F. Busnengo, DFT study of dissociative adsorption of hydrogen sulfide on Cu(111) and Au(111), Langmuir 24 (2008) 14022–14026.
- [23] P.J. Feibelman, Formation and diffusion of S-decorated Cu clusters on Cu(111), Phys. Rev. Lett. 85 (2000) 606–609.
- [24] Q.-L. Tang, S.-R. Zhang, Y.-P. Liang, Influence of step defects on the H_2S splitting on copper surfaces from first-principles microkinetic modeling, J. Phys. Chem. C 116 (2012) 20321–20331.
- [25] J.H. Stenlid, A.J. Johansson, C. Leygraf, T. Brinck, Computational analysis of the early stage of cuprous oxide sulphidation: a top-down process, Corros. Eng. Sci. Technol. 52 (2017) 50–53.
- [26] W. Heegemann, K.H. Meister, E. Bechtold, K. Hayek, The adsorption of sulfur on the (100) and (111) faces of platinum; a LEED and AES study, Surf. Sci. 49 (1975) 161–180.
- [27] G. Kresse, J. Furthmüller, Efficiency of ab-initio total energy calculations for metals and semiconductors using a plane-wave basis set, Comput. Mater. Sci. 6 (1996) 15–50.
- [28] G. Kresse, J. Furthmüller, Efficient iterative schemes for ab initio total-energy calculations using a plane-wave basis set, Phys. Rev. B 54 (1996) 11169.
- [29] G. Kresse, D. Joubert, From ultrasoft pseudopotentials to the projector augmented-wave method, Phys. Rev. B 59 (1999) 1758.
- [30] J.P. Perdew, J.A. Chevary, S.H. Vosko, K.A. Jackson, M.R. Pederson, D.J. Singh, C. Fiolhais, Atoms, molecules, solids, and surfaces: applications of the generalized gradient approximation for exchange and correlation, Phys. Rev. B 46 (1992) 6671–6687.
- [31] B. Eren, D. Zherebetskyy, L.L. Patera, C.H. Wu, H. Blum, C. Africh, L.-W. Wang, G.A. Somorjai, M. Salmeron, Activation of Cu(111) surface by decomposition into nanoclusters driven by CO adsorption, Science 351 (2016) 475–478.
- [32] K. Kern, H. Niehus, A. Schatz, P. Zeppenfeld, J. Goerge, G. Comsa, Long-range spatial self-organization in the adsorbate-induced restructuring of surfaces: Cu(100)-(2 \times 1)O, Phys. Rev. Lett. 67 (1991) 855–858.
- [33] Z. Pang, S. Dürrbeck, C. Kha, E. Bertel, G.A. Somorjai, M. Salmeron, Adsorption and reactions of water on oxygen-precovered Cu(110), J. Phys. Chem. C 120 (2016) 9218–9222.
- [34] R. Steudel, Properties of sulfur-sulfur bonds, Angew. Chem. Int. Ed. Engl. 14 (1975) 655–664.
- [35] R. Steudel, Y. Steudel, Polysulfide chemistry in sodium-sulfur batteries and related systems—a computational study by G3X(MP2) and PCM calculations, Chem.–Eur. J. 19 (2013) 3162–3176.
- [36] B.N. Frandsen, P.O. Wennberg, H.G. Kjaergaard, Identification of OSSO as a near-UV absorber in the Venusian atmosphere, Geophys. Res. Lett. 43 (2016) 11146–11155.